

MAGNET STRENGTH FLUCTUATIONS IN THE SSC LATTICE

PART 1: Zero Frequency Modulation

G.P.Goderre
Texas Accelerator Center
February 1987

Introduction

Tune shift, smear, and closed orbit variations caused by magnet strength fluctuations are studied using the SSC realistic lattice, with clustered-IR's. This lattice has a 60° phase advance per cell and is set up using collision optics. Magnet strength fluctuation is due to current modulation in the main power supplies. The SSC lattice consists of ten main power supplies to drive the superconducting dipole and quadrupole magnets. The effect of current modulation on each supply is examined separately. The particular power supply being studied has the magnetic field strength of all magnets connected to it modulated by $(\Delta B/B) \cos(\omega t)$ (where $\Delta B/B =$ fractional modulation amplitude), and all other magnets are unmodulated. The results presented in this report are for a modulation frequency of zero (i.e. $\omega = 0$; a current offset). Of the ten main power supplies there are four different magnet configurations to be studied which are the following:

- + 41 cell arc sector
- o 42 cell arc sector ($7 \times 2\pi$ phase advance)
- Δ low beta straight section
- \square medium beta straight section

The realistic lattice is the following combination of these configurations:

+ , o , o , + , \square , + , o , o , + , Δ .

Lattice Settings

Random errors are assigned to each dipole using a gaussian random number generator. The sigmas associated with the gaussian distribution for each of the multipole errors is given in Table 6. The zero amplitude tune is adjusted using the correction quadrupoles in the arc spools (one focusing and one defocusing quadrupole per cell). The main quadrupole strengths are fixed by the main power supply to which they are connected, and are modulated along with the main dipoles. For all of the results presented here the x-tune was set to 78.265 and the y-tune to 78.285. The chromaticity is adjusted using two families of sextupoles located in the arc spool pieces. The x and y chromaticity values are +0.003 and -0.00001 respectively. Horizontal and vertical motions are not decoupled in this calculation. Since there are no skew quadrupoles in the system and no solenoids in the IR's, the only source of coupling comes from higher order multipole feed down which is very small in our case.

Results

The linear tune shift is calculated using the 4×4 transfer matrix obtained from TEAPOT¹ for the following cases:

+ zero frequency modulation of a 41 cell arc sector

with errors	$\Delta\nu_{x,y}/(\Delta B/B) =$	$-14.2 \pm 5.4, -16.5 \pm 3.8$
without errors		$-15.3 \pm 0.1, -15.3 \pm 0.1$

o zero frequency modulation of a 42 cell arc sector

with errors	$\Delta\nu_{x,y}/(\Delta B/B) =$	$-16.5 \pm 2.1, -14.9 \pm 1.6$
without errors		$-15.7 \pm 0.1, -15.7 \pm 0.1$

Δ zero frequency modulation of the low beta straight section

with errors	$\Delta\nu_{x,y}/(\Delta B/B) =$	$+86.3,$	$+73.6$
without errors		$+88.3,$	$+71.6$

\square zero frequency modulation of the medium beta straight section

with errors	$\Delta\nu_{x,y}/(\Delta B/B) =$	$+38.9,$	$+25.3$
without errors		$+39.1,$	$+25.0$

Figure 1 shows that there is a linear relationship between tune and the amplitude of the modulation ($\Delta B/B$). So the results are quoted in terms of the ratio of the tune shift to the modulation amplitude. To get the tune shift for any modulation amplitude, it is only necessary to multiply by the modulation amplitude ($\Delta B/B$).

Table 1 is a tabulation of the tune when the zero frequency modulation is applied to different power supplies around the ring. Modulation of a 42 cell arc sector causes a slightly larger tune shift than the same modulation applied to a 41 cell arc sector. In the case without errors this difference is due to the larger number of cells in the 42 cell sector (see last row of table 1). Random errors in the dipoles cause fluctuations in the tune which are much greater than the per cell tune shift (i.e. $\Delta\nu_{x,y}/(\Delta B/B) = -0.4, -0.4$) caused by modulation. Therefore, when random errors are included, the difference between a 41 and a 42 cell sector is due to the choice of random seed, and is not affected by modulation. The tune shift per modulation amplitude due to modulation of a focusing and a defocusing quadrupole in an arc cell is approximately $+0.2$. This implies that the contribution of the chromaticity sextupoles to the tune is approximately -0.6 per cell in the arcs. Modulation of the straight sections has a much larger effect on the tune than modulation of an arc sector. This is due mostly to modulation of the IR quadrupoles, which shift the tune per modulation amplitude by $+58.55$ in the case of the low beta IR, and $+10.75$ in the case of the medium beta IR (see tables 5a and 5b). Since the sign of the tune shift in the straight sections is opposite that in the arcs, when all magnets are modulated the large shift in the straight sections is canceled by those in the arcs.

Table 1 shows that when all magnets are modulated, the tune is approximately equal to the sum of individual modulation of each power supply. This says that the size of the tune shift is highly dependent on the phasing of the modulation. If the phase of the modulation is zero then $\Delta\nu_{x,y}/(\Delta B/B) = 3.4, -27.3$ whereas if the phase of the straight section is 180° relative to the arcs these values become $\pm 247.9, \pm 224.6$. Further studies show that the assumption of simply adding the effects of individual power supplies may not be valid when the modulation frequency is other than zero. These studies will appear in a separate report.

The tune shift as a function of initial amplitude is obtained by tracking a particle for 512 turns with TEAPOT¹. The results of tracking are used to calculate the tune from the Fourier spectrum of the particle position at a beam pickup located in the arc, and the smear is calculated from the variation of the linear invariant ($W_{x,y}$). The tune shift ($\Delta\nu_{x,y}$) vs amplitude ($A_{x,y}^2$) and the smear ($S_{x,y}$) are evaluated for the following cases:

- no field strength fluctuations
- + zero frequency modulation of a 41 cell arc sector
- o zero frequency modulation of a 42 cell arc sector
- △ zero frequency modulation of the low beta straight section
- zero frequency modulation of the medium beta straight section

Figures 2a and 2b show the x-tune as a function of amplitude with and without random errors in the dipoles respectively. Figures 3a and 3b show the y-tune as a function of amplitude with and without random errors respectively. Without errors modulation has no effect on the variation of tune with amplitude (see figures 2b and 3b). The variation in tune with amplitude in this case is due to the chromaticity sextupoles (second order sextupole effect which is equivalent to a first order octupole). When random errors are included the linear relationship between the x-tune and A_x^2 breaks down for $A_x^2 > 0.15 \times 10^{-6} m^2$ at $\beta_x = 1m$. Even in the presence of random errors modulation appears to have little effect on the variation of tune with amplitude. The x-tune for both the 41 and 42 cell arc sectors drop more rapidly with amplitude in the nonlinear region (i.e. $W_x > 0.15 \times 10^{-6} m$) than any of the other cases (later it is found that the smear is also large for modulation in the arcs). The variation in tune with amplitude is due to the chromaticity sextupoles and the random errors in the dipoles. The contribution of the dipole errors to the tune shift with amplitude is approximately 30%. With random errors the y-tune variation with A_y^2 is very small and nonlinear for all amplitudes (compare figures 3a and 3b). All these data indicate that modulation has little or no effect on the relationship between tune and amplitude. Therefore, a DC current offset between power supplies should present no problems. Here again, studies (to appear in a later report) indicate that when the modulation frequency is not zero the phasing of the modulation between power supplies may become important. Then modulation may effect the variation of tune with amplitude. However, the results of the present study indicate that modulation should have little or no effect on the tune variation with amplitude.

Figures 4a and 4b show the x and y smear respectively. Here smear (S_s) is defined as follows:

$$S_x = 2 \cdot \frac{A_x^{max} - A_x^{min}}{A_x^{max} + A_x^{min}}$$

where

$$W_x = A_x^2 / \beta_x$$

$$A_x = \sqrt{z^2 + (\alpha_x z + \beta_x z')^2}$$

Examination of these figures indicates that the smear with random errors is slightly worse with modulation on an arc sector. Modulation degrades both the smear and tune variation with amplitude when applied to an arc sector.

The closed orbit x and y position is plotted as a function of the location around the ring (s) for the following cases:

- a) (+) modulation of a 41 cell sector
- b) (o) modulation of a 42 cell sector
- c) (Δ) modulation of low beta straight section
- d) (\square) modulation of medium beta straight section
- e) no modulation

The closed orbit (both x and y position) with no modulation is zero or very small for all positions (s) around the ring. This is true for both cases with and without random errors. So these plots have been suppressed. Figures 5a through 5d show the x-position of the closed orbit with random errors in the dipoles. Figure 5b shows that the perturbation of the orbit is localized when modulating a 42 cell sector. Figure 5a shows that when modulating a 41 cell sector the entire orbit is modified. Therefore, the effect of orbit distortion can be minimized by choosing the number of cells connected to a power supply, such that the phase advance is $n \times 2\pi$, where n is an integer (i.e. the supply drives an achromat). Figures 5c and 5d show that when modulating the straight sections, the orbit perturbation is moderately contained within the straight section being modulated. Notice that the largest orbit distortion occurs when modulating a 41 cell sector or the low beta straight section (figures 5a and 5c). In both cases the largest excursion is in the low beta straight section. Figures 7a through 7d show the x-position of the closed orbit without errors. Comparing these figures with figures 5a through 5d show that random errors have no noticeable effect on the x-position of the closed orbit.

Figures 6a through 6d show the y-position of the closed orbit including random errors. In all cases the deviation of the orbit is very small (less than $5\mu m$). The y-position of the closed orbit without errors is not shown since they are identically zero for all s with and without modulation.

Tune shift due to modulation of the IR trim quadrupoles is estimated by applying a zero frequency modulation to the IR focusing/defocusing quadrupoles. The amplitude of the modulation is 10% of what was used in the previous studies, since the trim quadrupoles are expected to contribute about 10% of the focusing power. The following cases are examined:

- 10% modulation on Q1 focusing/defocusing quadrupole
- 10% modulation on Q2 focusing/defocusing quadrupole
- 10% modulation on Q3 focusing/defocusing quadrupole
- 10% modulation on a single IR in a particular straight section
- 10% modulation on both IR's in a particular straight section

The tune for the various cases is tabulated in table 4. The analyses of these data are shown in tables 5a and 5b. Table 5b shows the tune shift for the above cases applied to the medium beta straight section, where the tune shift agrees with the simple formula $\Delta\nu = \frac{1}{4\pi}\beta k(\frac{\Delta k}{k})$. Table 5a shows the same results for modulation of the trim quadrupoles in the low beta straight section. The simple formula appears to overestimate the tune shift in the low beta IR's where interference effects are not negligible. The effect of modulating the IR trim quadrupoles by $\Delta B/B = 10^{-4}$ will modulate the tune by less than 0.001.

Summary

Tune shift modulation is highly dependent on the phasing of the modulation on the different power supplies. With modulation of $\Delta B/B < 10^{-5}$, the tune can vary between ± 0.00003 and ± 0.0025 . Here it has been assumed that the total tune shift is the sum of the contributions from modulating each power supply separately. Preliminary results indicate that this may not be true when the modulation frequency is not zero.

The change in tune with amplitude caused by the chromaticity sextupoles and random errors in the dipoles is not affected by power supply modulation in the static cases studied.

Modulation of the arc power supplies causes the largest increase in the smear. The combined effect of modulating all power supplies simultaneously with modulation frequencies other than zero were not studied to estimate the effect of the phasing of the modulation on the smear.

Closed orbit perturbations caused by the modulation are reduced, if the power supply is driving an achromat.

Tune variation due to modulation of the IR trim quadrupoles ($\Delta B/B < 10^{-6}$) is estimated to be less than 0.0001.

It should be noted that when all magnets are given an offset of $\Delta B/B = 10^{-4}$ (which is equivalent to $\Delta p/p = 10^{-4}$), $\Delta\nu_{x,y}/(\Delta B/B)$ is equal to +3.4 and -27.3 for x and y respectively. This does not seem to agree with the chromaticity settings of +0.003 and -0.00001 for x and y respectively.

FIGURE 1
 ν_x vs. $\frac{\Delta B}{B}$

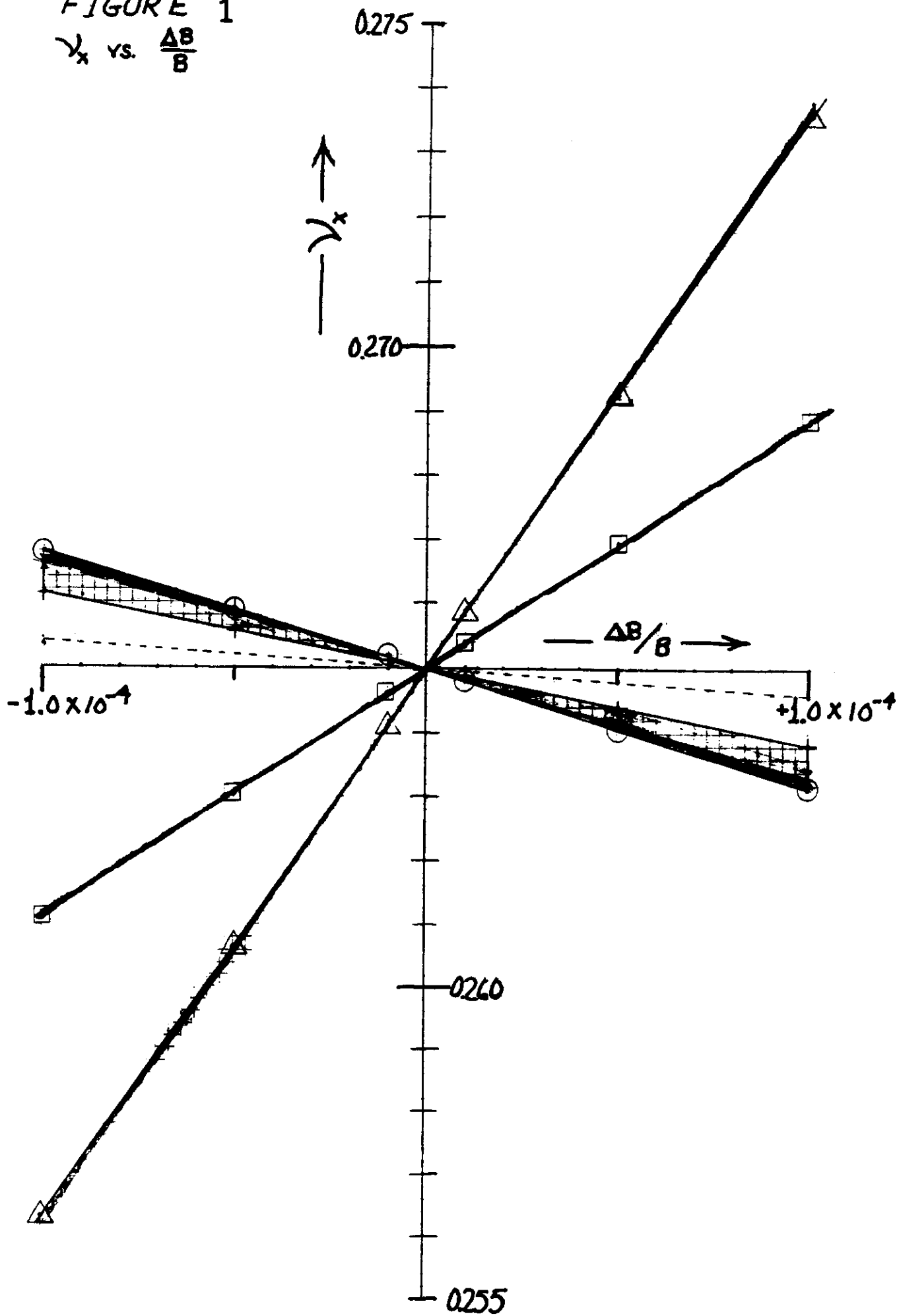


Figure 2a

x-fractional tune vs. W_x
with random errors in dipoles (tables)

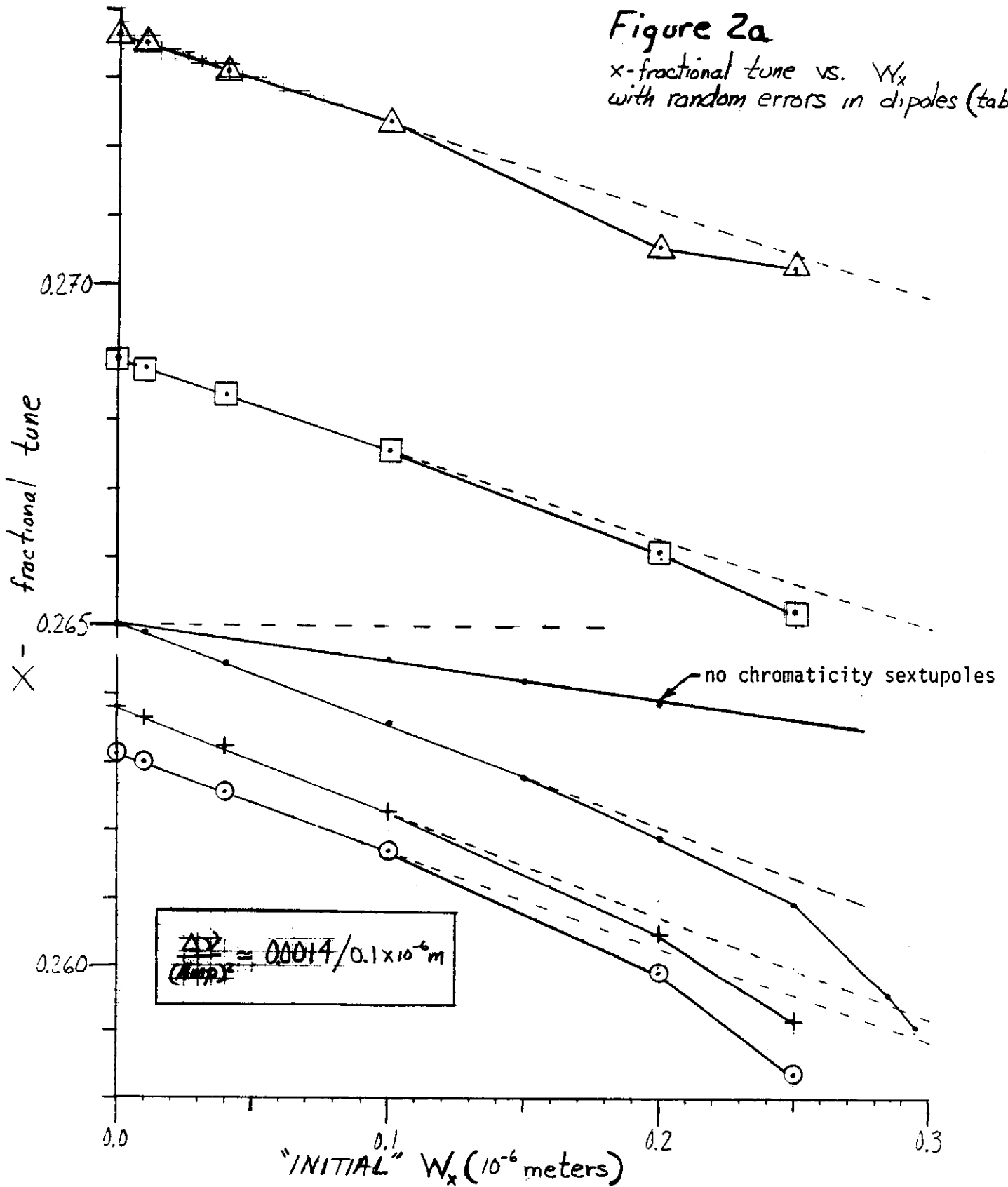


Figure 2b
 x-fractional tune vs. W_x
 without random errors

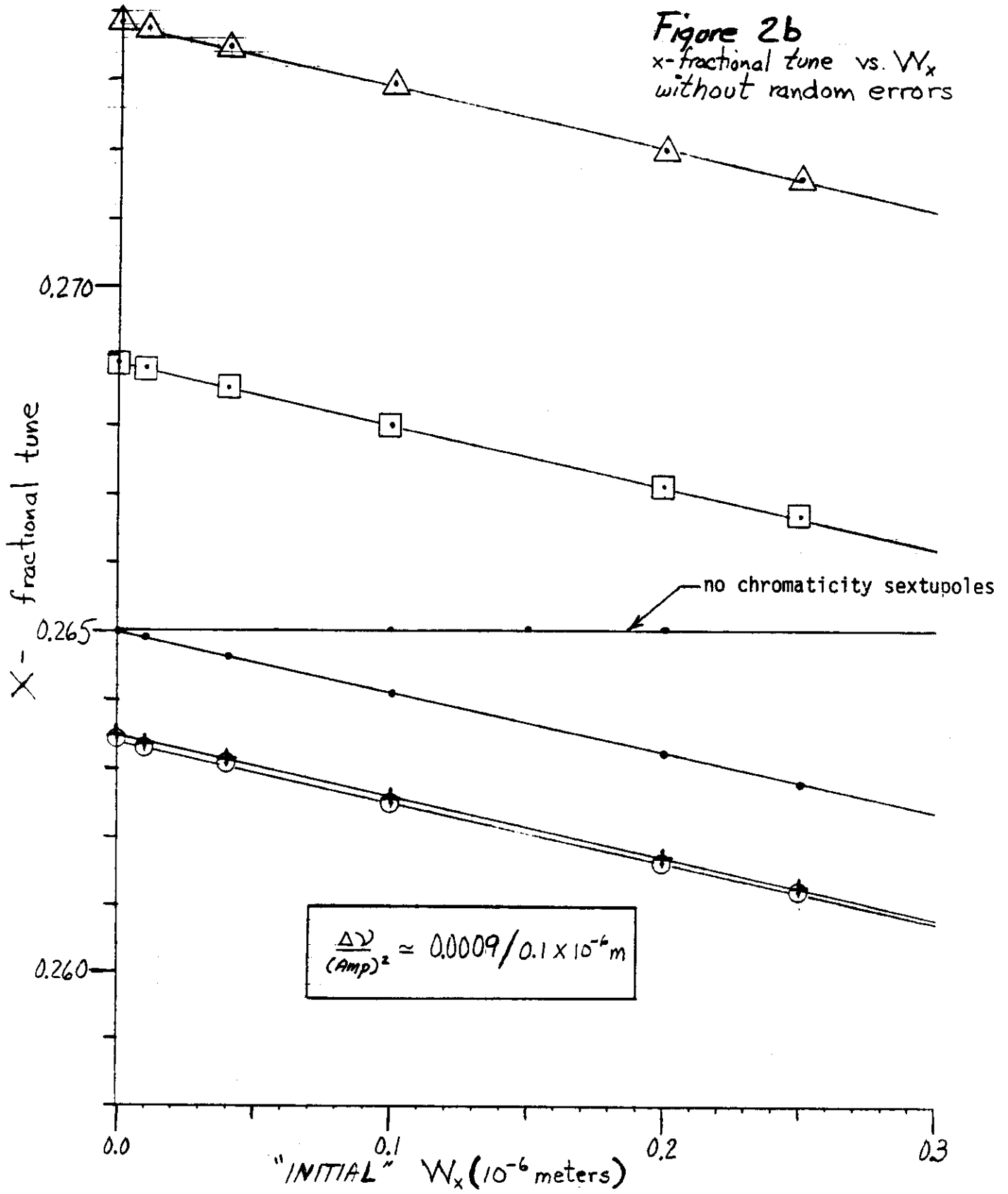


Figure 3a.

γ -fractional tune vs W_y
with random errors in dipoles (see table 6)

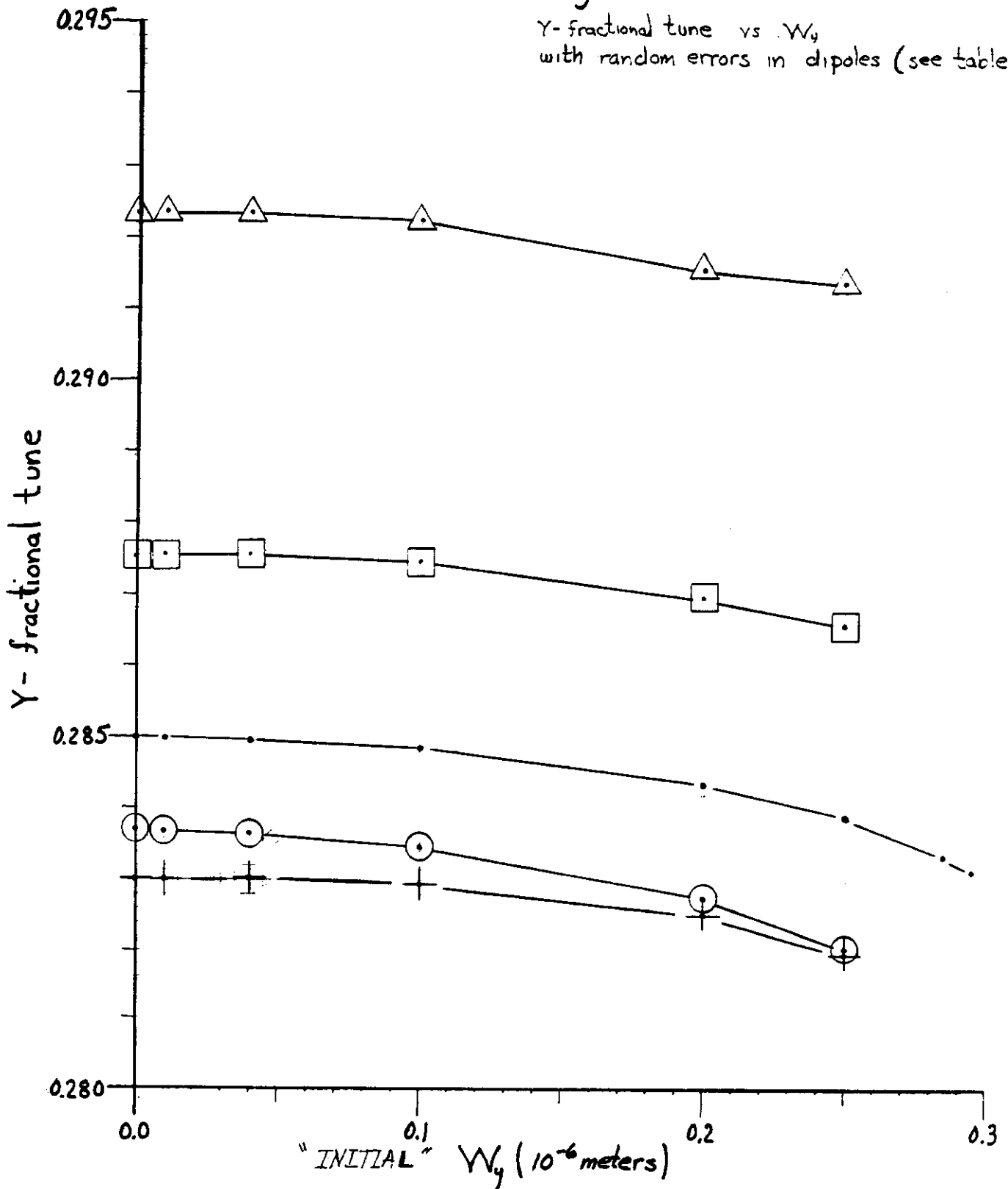
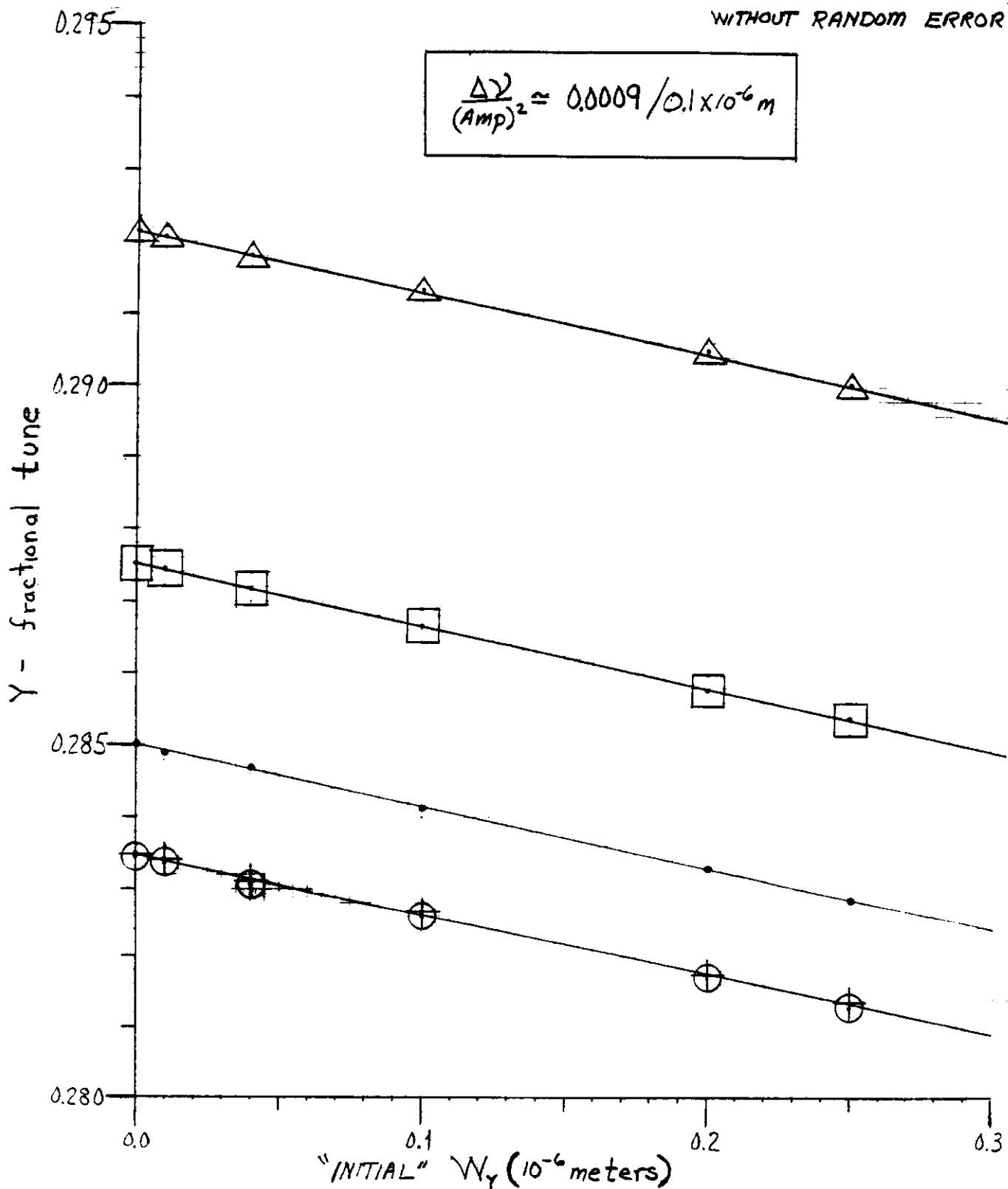


Figure 3b
 Y-fractional tune vs. W_y
 WITHOUT RANDOM ERRORS



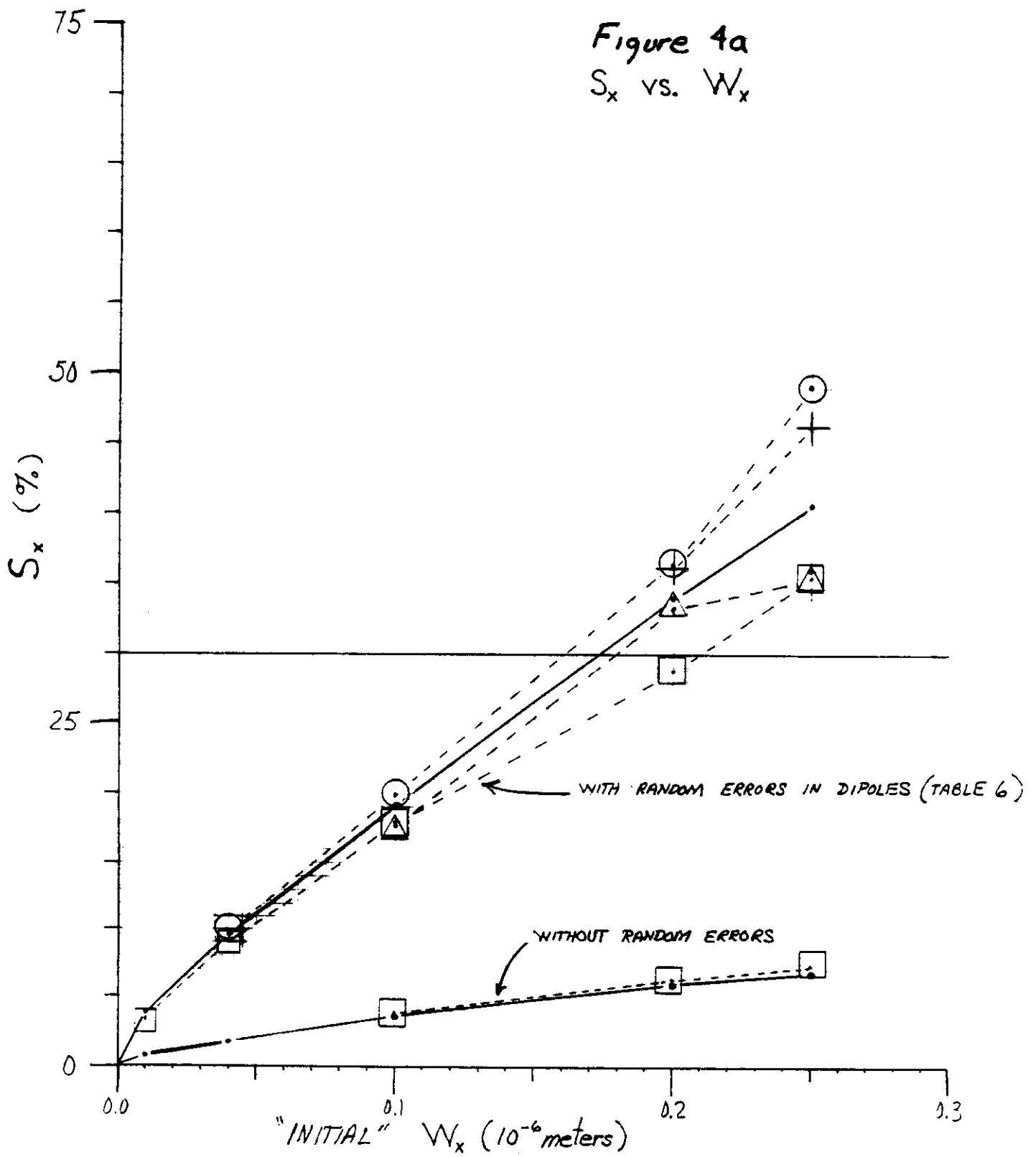
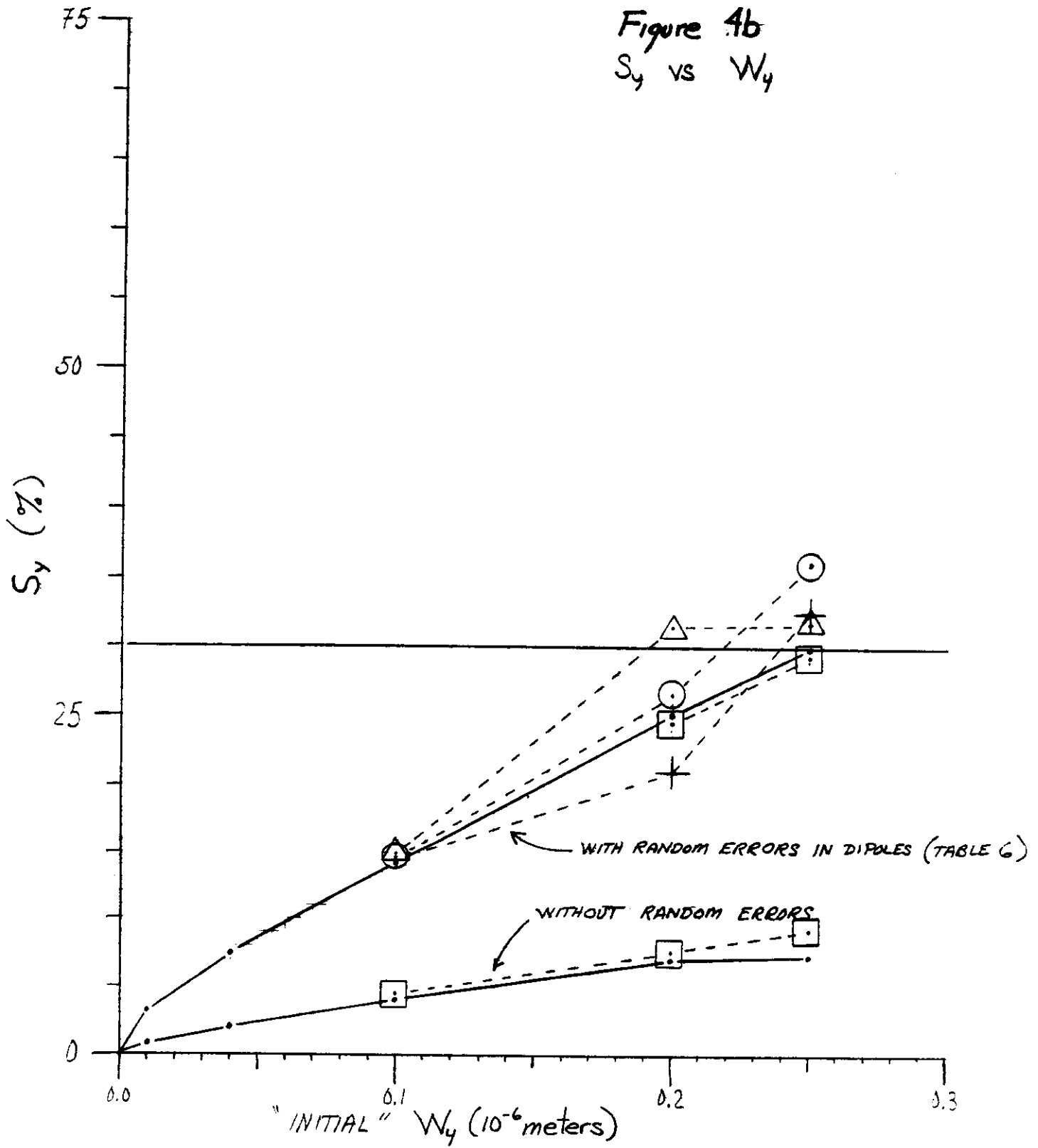
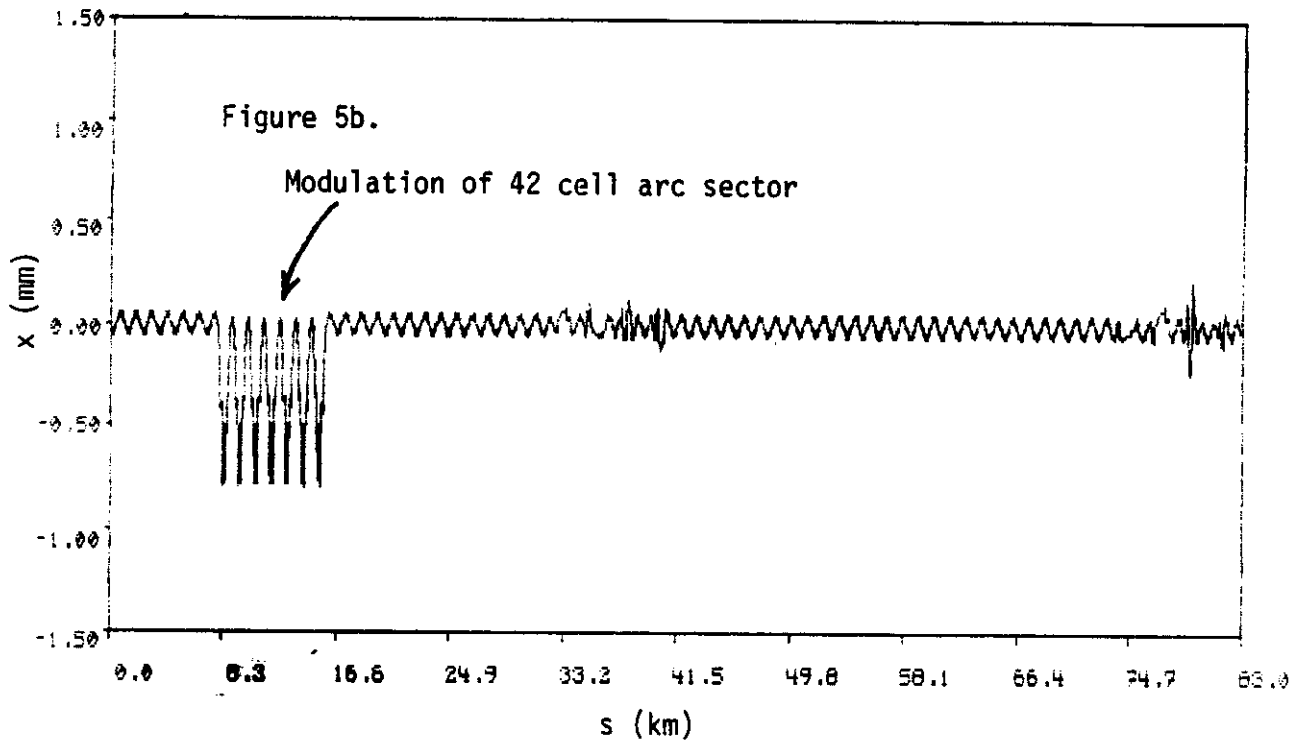
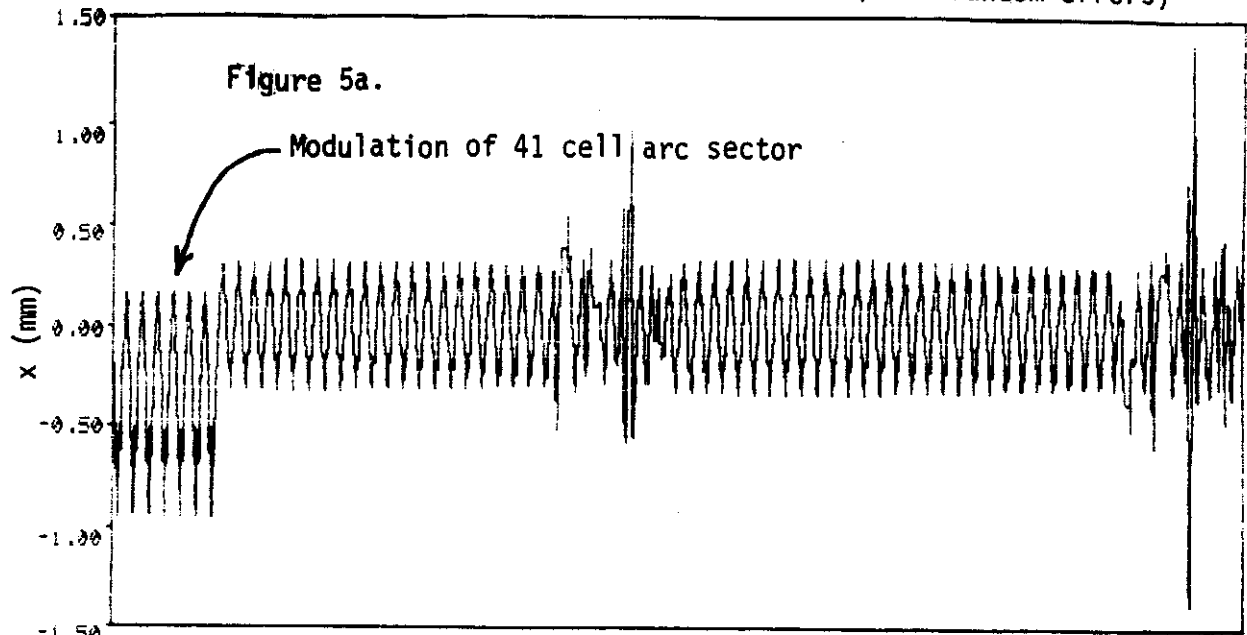


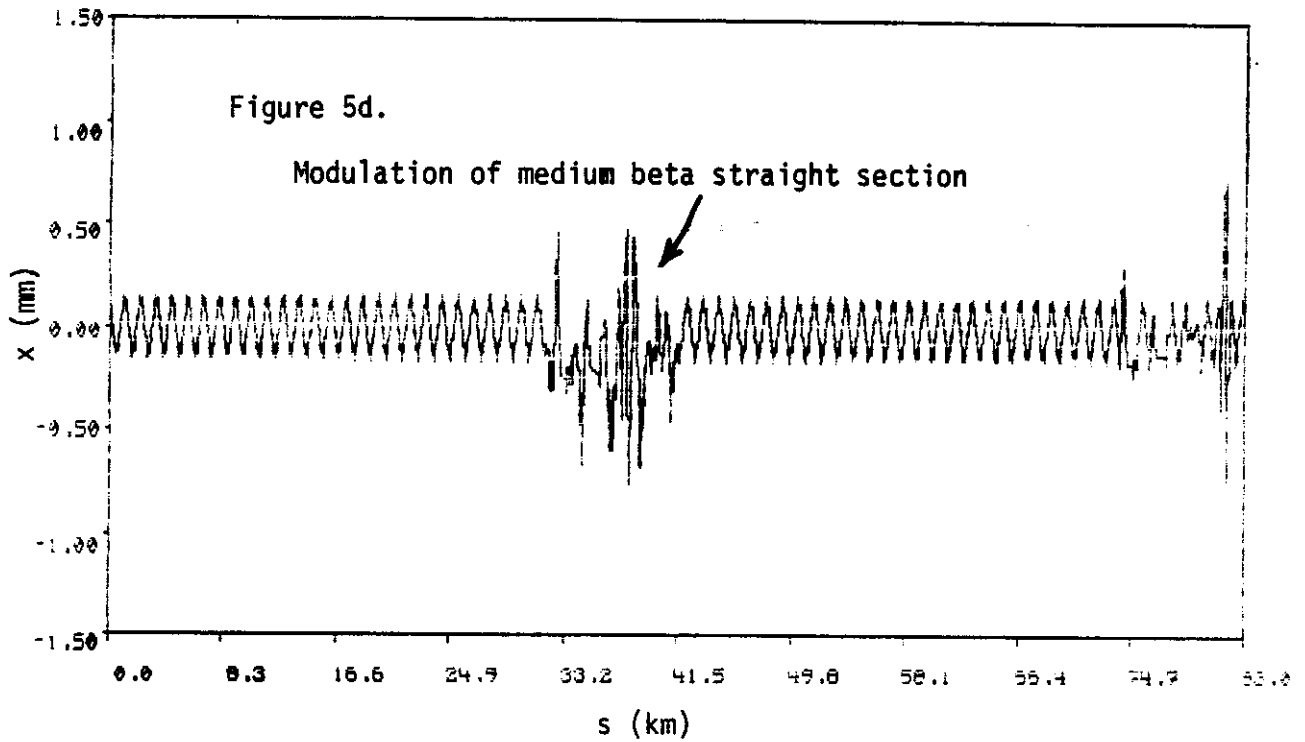
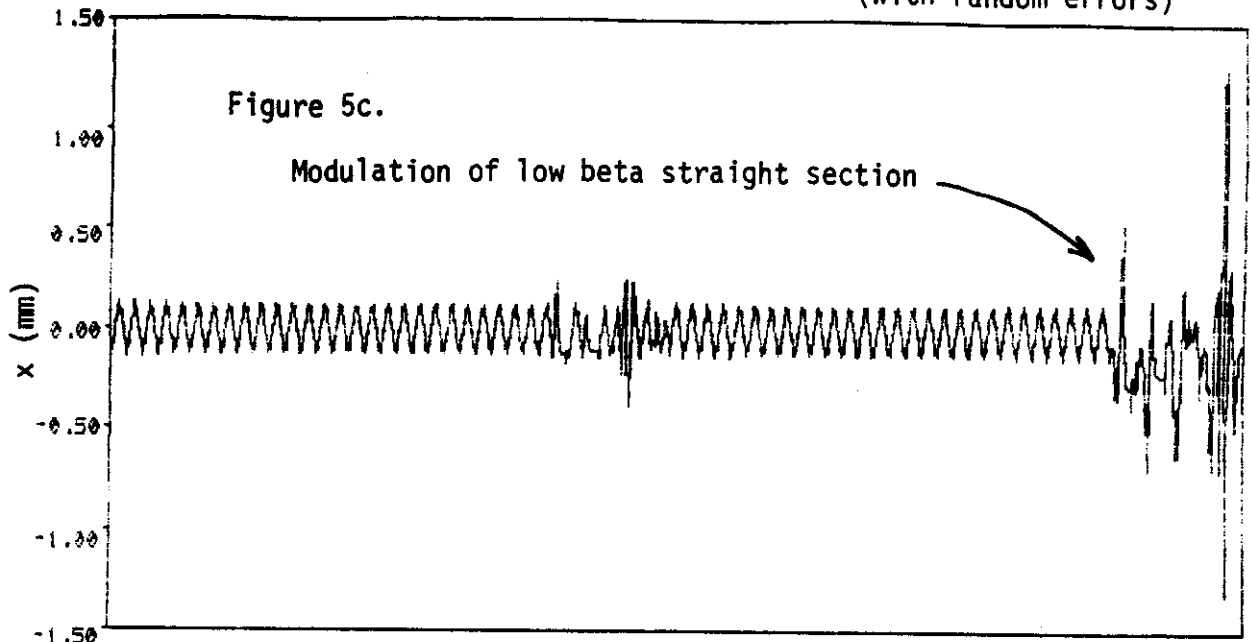
Figure 4b
 S_y vs W_y



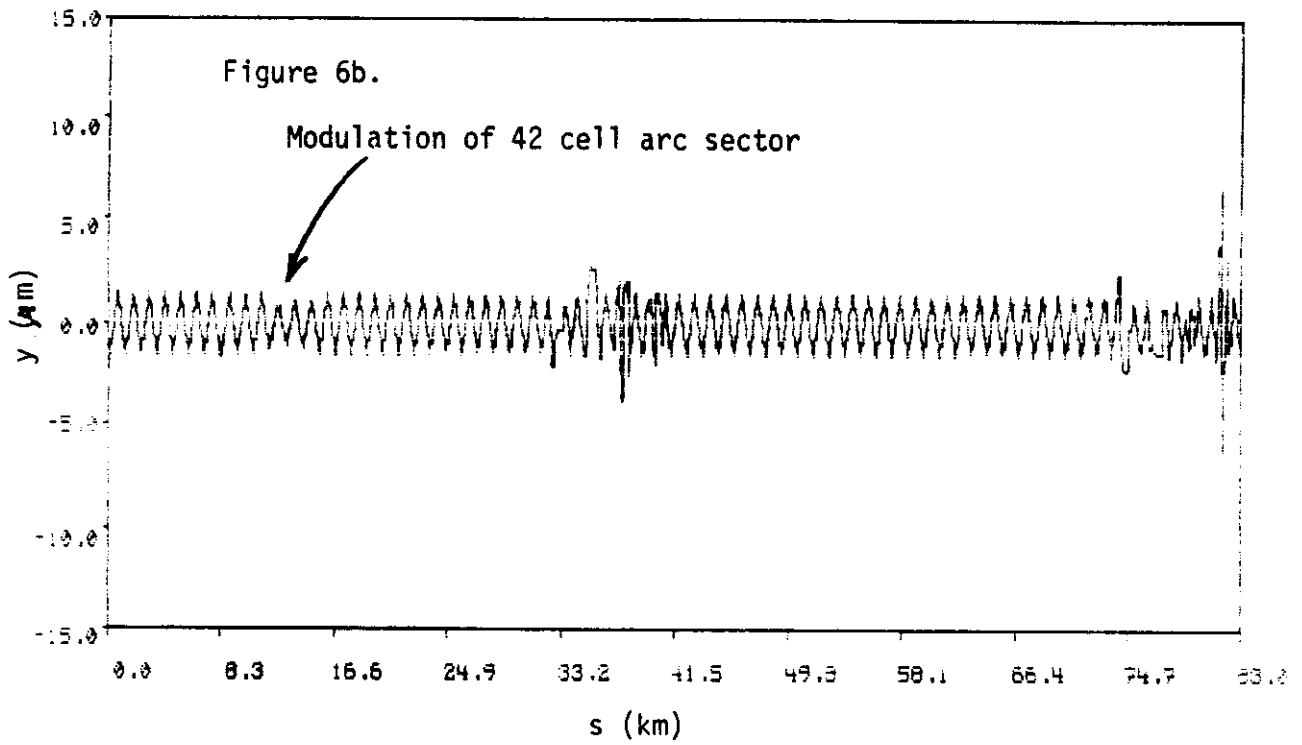
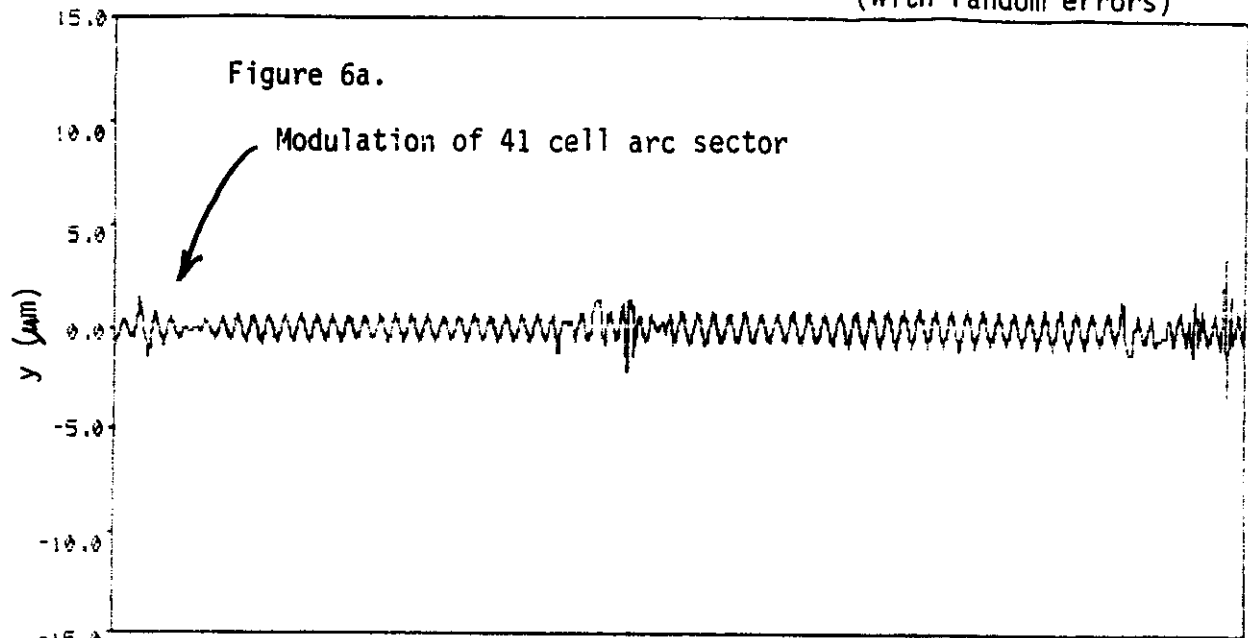
X - CLOSED ORBIT (with random errors)



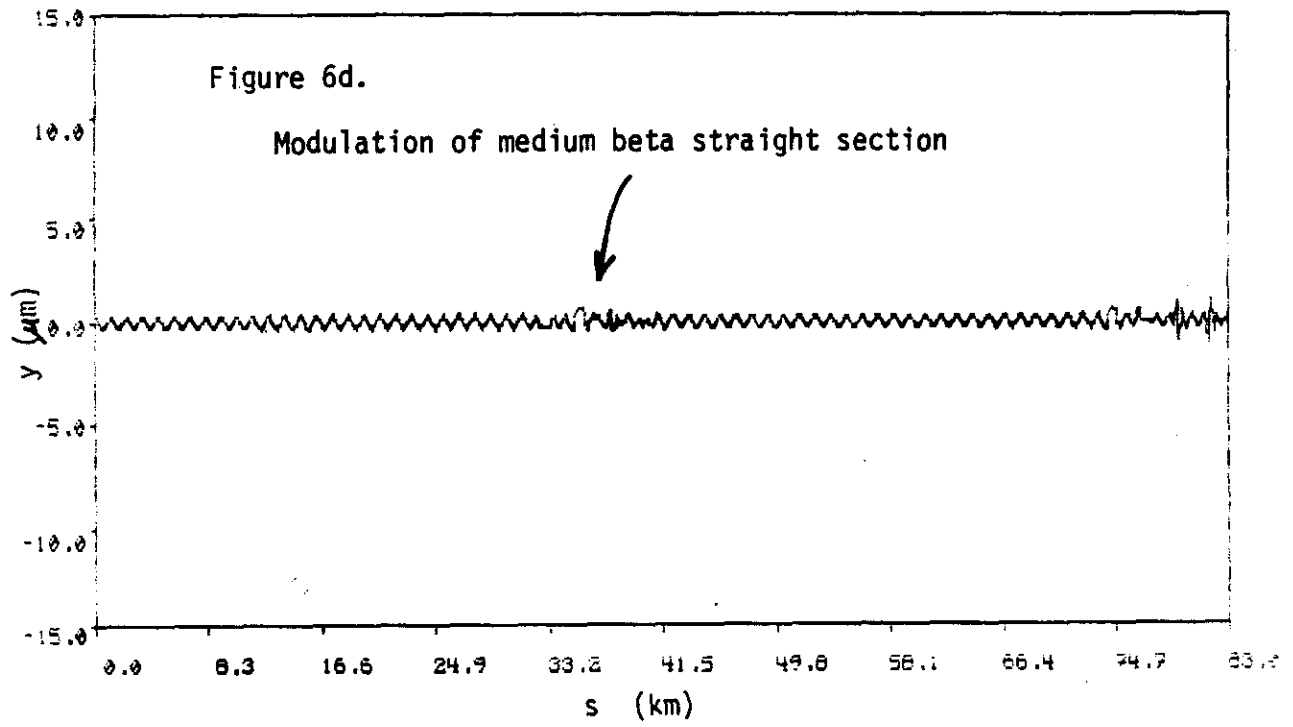
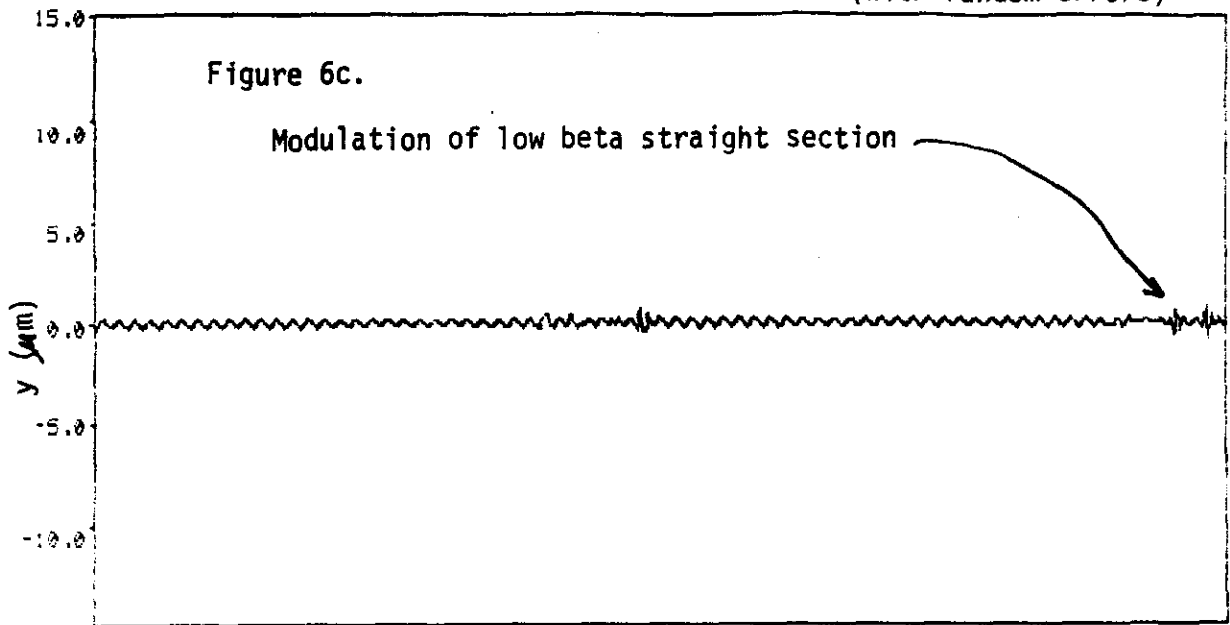
X - CLOSED ORBIT (with random errors)



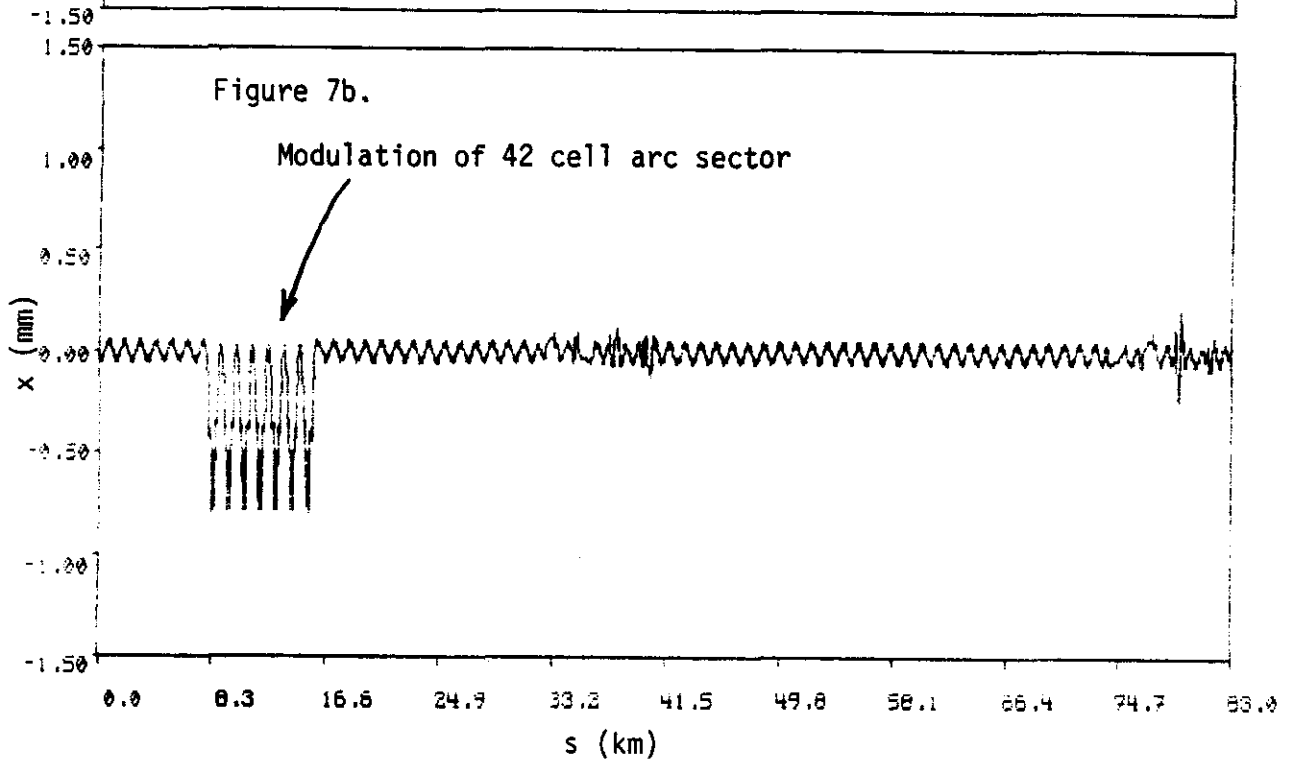
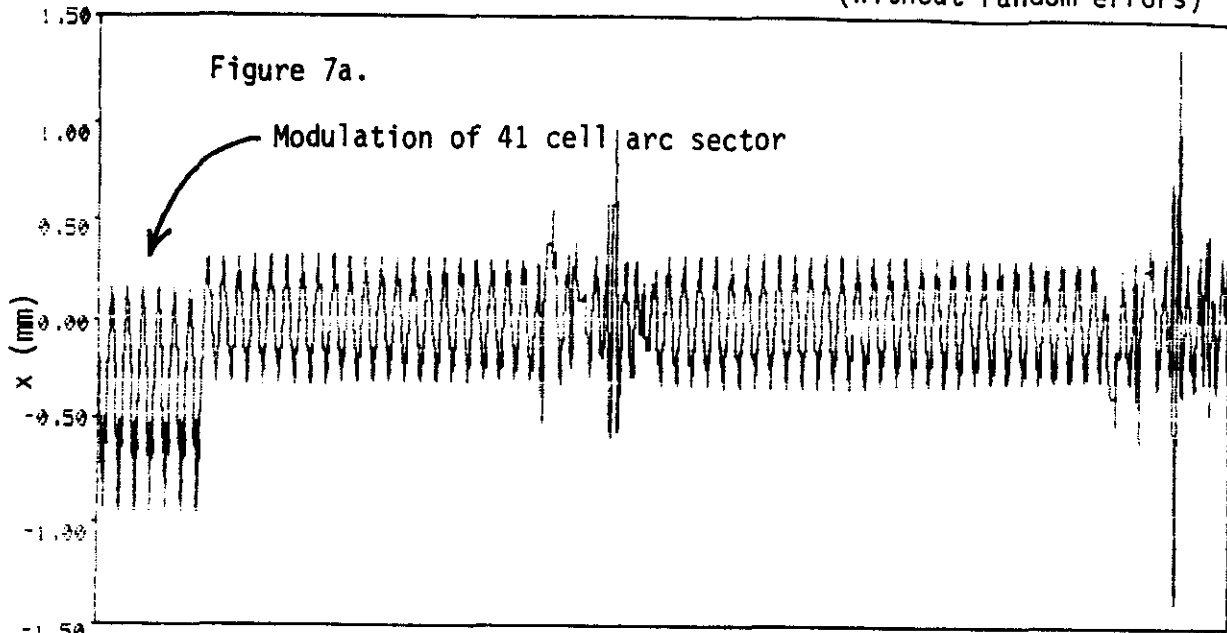
Y - CLOSED ORBIT (with random errors)



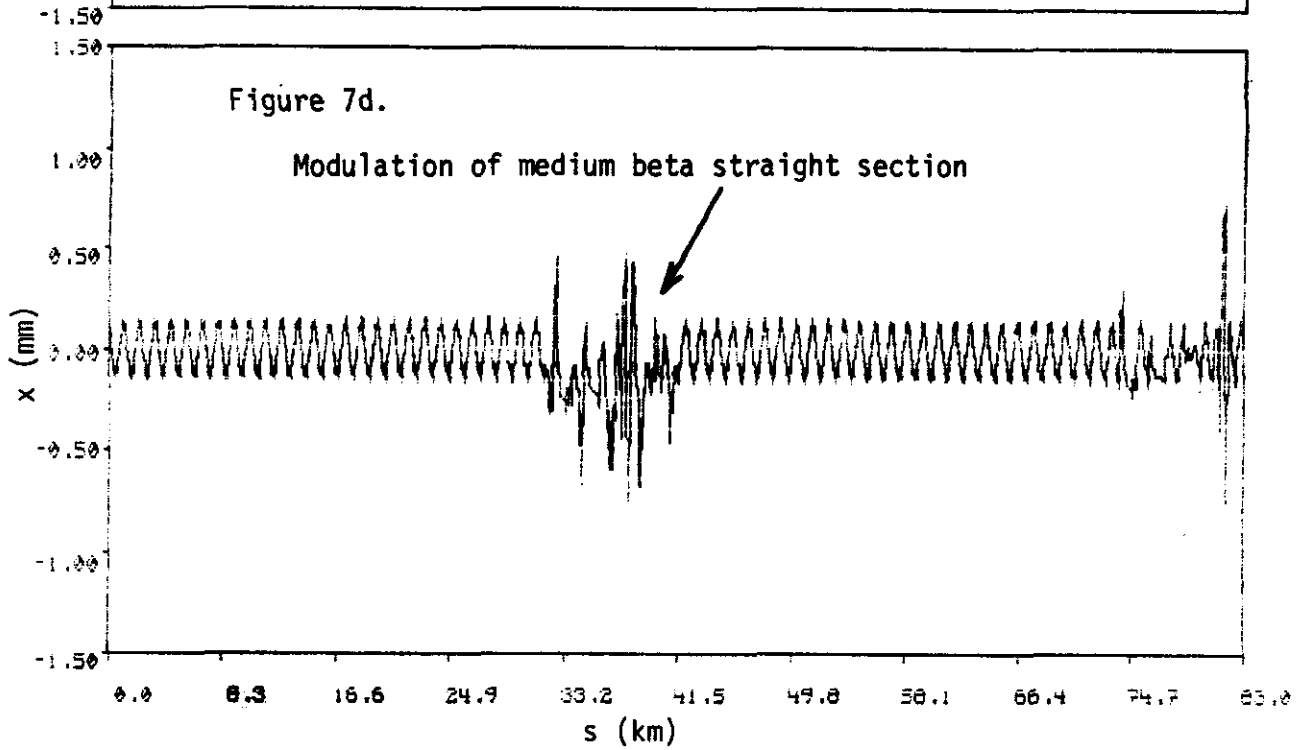
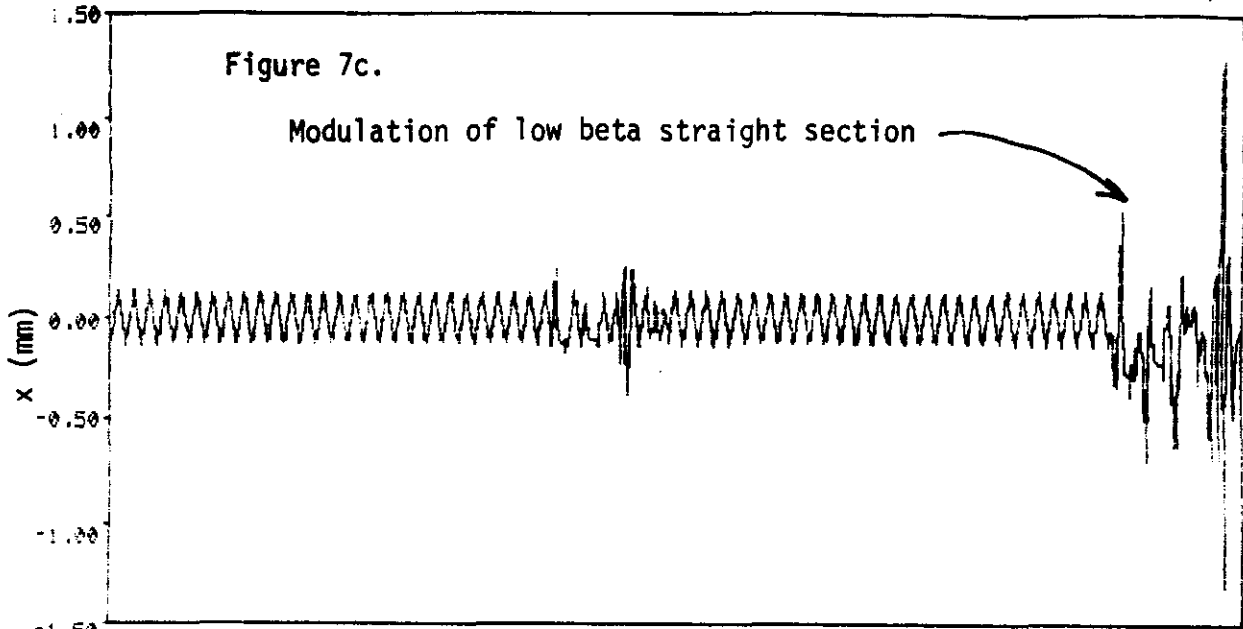
Y - CLOSED ORBIT (with random errors)



X - CLOSED ORBIT (without random errors)



X - CLOSED ORBIT (without random errors)



$$\frac{\Delta B}{B} = 10^{-4}$$

Table 1

SECTOR	CONFIGURATION	WITH RANDOM ERRORS		WITHOUT RANDOM ERRORS	
		V_x ΔV_x	V_y ΔV_y	V_x ΔV_x	V_y ΔV_y
1	+	0.26380177 0.26380177	0.28301123 +1.95 x 10⁻³	0.26348 +1.52 x 10⁻³	0.28347 +1.53 x 10⁻³
2	⊙	0.26311543 -1.89×10^{-3}	0.28369598 -1.30×10^{-3}	0.26343 -1.57×10^{-3}	0.28343 -1.57×10^{-3}
3	⊙	0.26325329 -1.75×10^{-3}	0.28354669 -1.45×10^{-3}	0.26342535 -1.58×10^{-3}	0.28342855 -1.57×10^{-3}
4	+	0.26323465 +1.77 x 10⁻³	0.28359068 +1.99 x 10⁻³	0.26346141 +1.54 x 10⁻³	0.28347828 +1.52 x 10⁻³
5	+	0.26304991 +1.95 x 10⁻³	0.28375233 +1.95 x 10⁻³	0.26347432 +1.53 x 10⁻³	0.28345117 +1.53 x 10⁻³
6	⊙	0.26347921 -1.52×10^{-3}	0.28346347 -1.54×10^{-3}	0.26342873 -1.57×10^{-3}	0.28342519 -1.58×10^{-3}
7	⊙	0.26358178 -1.42×10^{-3}	0.28332683 -1.67×10^{-3}	0.26342897 -1.57×10^{-3}	0.28342584 -1.57×10^{-3}
8	+	0.26423340 +2.17 x 10⁻³	0.28304107 +1.99 x 10⁻³	0.26348509 +1.52 x 10⁻³	0.28348148 +1.52 x 10⁻³
9	△	0.27362896 $+8.63 \times 10^{-3}$	0.29236410 $+7.36 \times 10^{-3}$	0.27383 $+8.83 \times 10^{-3}$	0.29216 $+7.16 \times 10^{-3}$
10	□	0.26888724 +3.89 x 10⁻³	0.28753012 +1.95 x 10⁻³	0.26891 +1.52 x 10⁻³	0.28750 +2.50 x 10⁻³
SUM		$+0.25 \times 10^{-3}$	-2.68×10^{-3}	$+0.34 \times 10^{-3}$	-2.75×10^{-3}
ALL		0.26534384 $+0.34 \times 10^{-3}$	0.28227133 -2.73×10^{-3}	0.26536015 $+0.36 \times 10^{-3}$	0.28226158 -2.74×10^{-3}
NONE		0.26500099 0.00×10^{-3}	0.28500017 0.00×10^{-3}	0.26500047 0.00×10^{-3}	0.28500031 0.00×10^{-3}
Average Arc	+	0.26380177	+1.95 x 10⁻³	+1.53 x 10⁻³	+1.53 x 10⁻³
	⊙	-1.65×10^{-3}	-1.49×10^{-3}	-1.57×10^{-3}	-1.57×10^{-3}
per cell		-0.04×10^{-3}	-0.04×10^{-3}	-0.04×10^{-3}	-0.04×10^{-3}

Table 2
"Data plotted in figure 1a,b"

SECTOR	CONFIGURATION	$\frac{\Delta B}{B}$ (10^{-4})	WITH RANDOM ERRORS		
			v_x	v_y	
1	+	1.0	0.26380177	0.28301123	0.0
		0.5	0.26440876	0.28400490	0.0
		0.1	0.26488363	0.28480104	0.0
		-0.1	0.26511785	0.28519931	0.1
		-0.5	0.26558053	0.28599594	0.1
		-1.0	0.26614935	0.28699112	0.1
2	⊙	1.0	0.26311543	0.28369598	0.0
		0.5	0.26406553	0.28434229	0.0
		0.1	0.26481522	0.28486761	0.0
		-0.1	0.26518606	0.28513324	0.1
		-0.5	0.26591878	0.28567087	0.1
		-1.0	0.26681595	0.28635562	0.1
9	△	1.0	0.27362896	0.29236410	0.0
		0.5	0.26932324	0.28868102	0.0
		0.1	0.26586693	0.28573620	0.0
		-0.1	0.26413425	0.28426418	0.1
		-0.5	0.26065869	0.28132067	0.1
		-1.0	0.25629272	0.27764178	0.1
10	□	1.0	0.26888724	0.28753012	0.0
		0.5	0.26694575	0.28626433	0.0
		0.1	0.26539017	0.28525291	0.0
		-0.1	0.26461172	0.28474745	0.1
		-0.5	0.26305379	0.28373676	0.1
		-1.0	0.26110488	0.28247333	0.1
ALL		1.0	0.26534384	0.28227133	
		-1.0	0.26457533	0.28772919	0.2
NONE		0.0	0.26500010	0.28500017	

Table 3

Data plotted in figure 2a through 4b

	$Y_{x,y}$ $10^{-6} m$	X-tune		Y-tune		S_x		S_y	
		WITHOUT RANDOMS	WITH RANDOMS	WITHOUT RANDOMS	WITH RANDOMS	WITHOUT RANDOMS	WITH RANDOMS	WITHOUT RANDOMS	WITH RANDOMS
NO BUMP •	0.00	0.26500	0.26500	0.28500	0.28500	—	—	—	—
	0.01	0.26493	0.26489	0.28490	0.28499	0.7	3.9	0.8	3.3
	0.04	0.26464	0.26444	0.28467	0.28497	1.8	9.7	2.1	7.4
	0.10	0.26412	0.26358	0.28416	0.28486	3.5	19.2	4.1	14.3
	0.20	0.26322	0.26189	0.28331	0.28437	5.9	34.0	7.0	25.3
	0.25	0.26281	0.26093	0.28284	0.28390	6.6	40.6	7.2	29.9
BUMP in Sector #1 +	0.00	0.26348	0.26380	0.28347	0.28301	—	—	—	—
	0.01	0.26337	0.26366	0.28341	0.28301	0.7	3.9	0.8	3.1
	0.04	0.26314	0.26322	0.28313	0.28303	1.7	9.9	2.1	7.0
	0.10	0.26258	0.26228	0.28265	0.28296	3.4	19.4	4.0	14.3
	0.20	0.26172	0.26048	0.28176	0.28253	5.9	36.2	6.9	21.0
	0.25	0.26127	0.25918	0.28134	0.28197	6.9	46.2	8.2	32.6
BUMP in Sector #2 ○	0.00	0.26343	0.26312	0.28343	0.28370	—	—	—	—
	0.01	0.26332	0.26301	0.28336	0.28368	0.7	3.9	0.8	3.9
	0.04	0.26308	0.26257	0.28308	0.28364	1.8	9.9	2.1	7.6
	0.10	0.26252	0.26169	0.28261	0.28345	3.5	19.8	4.0	14.5
	0.20	0.26165	0.25990	0.28173	0.28274	5.9	36.4	7.0	26.6
	0.25	0.26122	0.25837	0.28129	0.28205	7.0	49.2	8.5	36.3
BUMP in Low Beta △	0.00	0.27383	0.27363	0.29216	0.29236	—	—	—	—
	0.01	0.27376	0.27351	0.29208	0.29238	0.8	4.1	0.9	3.5
	0.04	0.27347	0.27311	0.29180	0.29236	1.9	9.5	2.2	7.8
	0.10	0.27294	0.27235	0.29134	0.29225	3.7	17.7	4.4	14.8
	0.20	0.27205	0.27056	0.29047	0.29158	6.1	33.3	7.0	31.4
	0.25	0.27165	0.27027	0.29002	0.29139	7.4	36.1	9.3	31.7
BUMP in Med Beta □	0.00	0.26891	0.26889	0.28750	0.28753	—	—	—	—
	0.01	0.26884	0.26878	0.28744	0.28755	0.7	3.6	0.9	3.3
	0.04	0.26855	0.26835	0.28717	0.28754	1.9	9.1	1.9	7.2
	0.10	0.26803	0.26756	0.28665	0.28746	3.7	17.9	4.3	14.0
	0.20	0.26714	0.26610	0.28578	0.28697	6.3	28.8	7.5	24.6
	0.25	0.26673	0.26522	0.28538	0.28659	7.4	35.5	9.0	29.3

Table 4

IR TRIM QUAD'S (Modulation $\frac{\Delta k}{k} = 10^{-5}$)
with random errors

	x-fractional tune	y-fractional tune
NO BUMP	0.26500099	0.28500017

BUMP IN LOW BETA

Q1 focusing	0.26503892	0.28493973
defocusing	0.26494183	0.28503815
one IR	0.26497976	0.28497770
both IR's	0.26495703	0.28495624

Q2 defocusing	0.26489823	0.28533657
focusing	0.26533106	0.28489641
one IR	0.26522826	0.28523276
both IR's	0.26546303	0.28546180

Q3 focusing	0.26518598	0.28489655
defocusing	0.26489913	0.28518752
one IR	0.26508411	0.28508388
both IR's	0.26516854	0.28516757

BUMP IN MED BETA

Q1 focusing	0.26502645	0.28497108
defocusing	0.26497158	0.28502401
one IR	0.26499704	0.28499492
both IR's	0.26499205	0.28499118

Q2 defocusing	0.26497683	0.28509878
focusing	0.26510100	0.28497737
one IR	0.26507683	0.28507598
both IR's	0.26515106	0.28515016

Q3 focusing	0.26501653	0.28496829
defocusing	0.26496859	0.28501493
one IR	0.26498413	0.28498305
both IR's	0.26496740	0.28496658

Table 5a)

WITH RANDOM ERRORS

Low Beta	β_x^{avg} (m)	$k=K1-L1$	$\frac{\Delta V_{cal}}{(\frac{\Delta K}{K})}$	$\frac{\Delta V_{meas}}{(\frac{\Delta K}{K})}$	% Difference
	TEAPOT	TEAPOT	$\frac{1}{4\pi} \beta k$	TEAPOT	
Q3f-a	5555.51	0.04405	19.47	18.50	5.2
Q2d-a	1725.71	-0.08356	-11.47	-10.28	11.6
Q1f-a	983.81	0.04892	3.83	3.79	1.1
mip	0.63				
Q1d-a	1533.93	-0.04892	-5.97	-5.92	0.8
Q2f-a	5541.11	0.08356	36.85	33.01	11.6
Q3d-a	3059.05	-0.04405	-10.72	-10.19	5.2
Q3-IR-a	—	—	8.75	8.31	5.2
Q2-IR-a	—	—	25.38	22.73	11.6
Q3-IR-a	—	—	-2.14	-2.13	0.5
Q3f-b	5575.01	0.04405	19.54	—	—
Q2d-b	1718.27	-0.08356	-11.43	—	—
Q1f-b	975.02	0.04892	3.80	—	—
mip	0.63				
Q1d-b	1554.44	-0.04892	-6.05	—	—
Q2f-b	5599.33	0.08356	37.23	—	—
Q3d-b	3085.06	-0.04405	-10.81	—	—
Q3-IR-b	—	—	8.73	—	—
Q2-IR-b	—	—	25.80	—	—
Q1-IR-b	—	—	-2.25	—	—
Q3-both IR's	—	—	17.48	16.75	4.3
Q2-both IR's	—	—	51.18	46.20	10.8
Q1-both IR's	—	—	-4.39	-4.40	0.2
			64.27	58.55	

Table 5b)

WITH RANDOM ERRORS

Med Beta	β_{x-}^{avg} TEAPOT	$k=K1 \cdot L1$ TEAPOT	$\frac{\Delta \chi_{cal}}{4\pi \beta k} / (\frac{\Delta k}{k})$	$\frac{\Delta \chi_{obs}}{TEAPOT} / (\frac{\Delta k}{k})$	% Difference
Q3f-a	939.93	0.02063	1.54	1.55	0.6
Q2d-a	676.40	0.04456	-2.40	-2.42	0.8
Q1f-a	1100.09	0.02887	2.53	2.55	0.8
mip	9.70				
Q1d-a	1273.48	0.02887	-2.92	-2.94	0.7
Q2f-a	2804.85	0.04456	9.95	10.00	0.5
Q3d-a	1963.01	0.02063	-3.22	-3.24	0.6
Q3-IR-a	————	————	-1.68	-1.69	0.6
Q2-IR-a	————	————	7.55	7.58	0.4
Q1-IR-a	————	————	-0.37	-0.40	7.5
Q3f-b	892.45	0.02063	1.46	—	—
Q2d-b	638.42	0.04456	-2.26	—	—
Q1f-b	1032.26	0.02887	2.37	—	—
mip	10.06				
Q1d-b	1248.97	0.02887	-2.87	—	—
Q2f-b	2744.00	0.04456	9.73	—	—
Q3d-b	1917.00	0.02063	-3.15	—	—
Q3-IR-b	————	————	-1.69	—	—
Q2-IR-b	————	————	7.47	—	—
Q1-IR-b	————	————	-0.50	—	—
Q3-both IR's	————	————	-3.37	-3.36	0.3
Q2-both IR's	————	————	15.02	15.01	0.1
Q1-both IR's	————	————	-0.87	-0.90	3.3
			10.73	10.75	

Table 6.) random errors in the dipole magnets

n	a_n $10^{-4}/\text{cm}^n$	b_n $10^{-4}/\text{cm}^n$
0	—	—
1	—	—
2	0.61	0.40 *
3	0.69	0.35
4	0.14	0.59
5	0.16	0.059
6	0.034	0.075
7	0.030	0.016
8	0.0064	0.021
9	0.0056	0.003

← these values were exchanged so that
 $a_6 = 0.075$, $b_6 = 0.034$

* b_2 is an effective value taking into account binning of magnets